International Journal of Aeronautical and Space Sciences (2019) 20:249–259
https://doi.org/10.1007/s42405-018-0106-3

IJASS International Journal of Aeronautical and Space Sciences

ORIGINAL PAPER

Demonstration of Active Vibration Control System on a Korean Utility Helicopter

Do-Hyung Kim[1] · Dong-Il Kwak[2] · Qi Song[3]

Received: 6 September 2018 / Accepted: 2 November 2018 / Published online: 10 November 2018

Abstract
Technology demonstration program was performed between June 2013 and January 2014 in Sacheon Korea to validate the performance of LORD Corporation (LORD)-designed active vibration control system (AVCS) on Korean Utility Helicopter platform. Optimal configuration of actuators was investigated by numerical calculation using ground and flight test data, and its performance was evaluated through the flight tests. 14 control accelerometers were used for vibration-level measurement and optimal configuration of 2–6 circular force generator test groups was investigated. Although the predicted vibration levels of aircraft showed better performance with increasing number of actuators, the weight and cost trade-off should be considered during the design. Flight tests showed that the vibration levels with AVCS at the cockpit area and the cabin area were reduced more than that of the tuned vibration absorber (TVA). Moreover, it was possible to configure AVCS with lower weight than the TVA.

Keywords Active vibration control system (AVCS) · Korean Utility Helicopter (KUH) · Circular force generator (CFG) · Optimization

1 Introduction

The main tonal vibration sources in the helicopter are rotating equipment, transmission, tail rotor and main rotor. The weight unbalance of the rotating equipment and the excessive vibration due to the gear meshing of the transmission can be prevented by design, precision machining and proper maintenance. It is possible to reduce the magnitude of the vibration from the tail rotor through balancing. In addition, the frequency band of the rotating tail rotor is higher than that of the rotating main rotor, and the induced vibration level is lower than that of the main rotor. Therefore, helicopter designers have mainly focused on the vibration induced by main rotor. The unsteady aerodynamic loading on the rotating main rotor is transmitted to the fuselage vibration through the hub, and the major frequency component of vibration transmitted to the non-rotating coordinate system is N/rev, which "N" is the number of blades [1–3]. The most basic aircraft design aspect is to avoid the resonance of the airframe and aircraft main component structures at the N/rev frequency, and the main structure of the KUH was also designed to avoid the 4/rev frequency (the KUH has 4 blades) [4]. In addition to structural design, there are passive and active technical approaches for further vibration reduction. Passive vibration reduction technique refers to absorbing or isolating vibration by generating a force or motion on the fuselage opposite to vibration without external energy input. Active vibration reduction method cancels vibration by generating controllable counter-acting force on the fuselage against vibration using external energy. In conventional helicopters deigned prior to the year 2005, passive vibration reduction devices have been mainly used. For example, absorbers are installed on the rotor head which is considered as the vibration source, isolators have been utilized in the vibration transfer path, and absorbers have also been applied to specific locations of airframe. Passive vibration reduction devices can be tuned at specific frequencies, but have limitations in terms of weight and drag and are also

Presented at the 7th Asian/Australian Rotorcraft Forum, Jeju Island, Korea, Oct. 30–Nov. 1, 2018.

✉ Do-Hyung Kim
dhkim@kari.re.kr

[1] Aircraft System Division, Korea Aerospace Research Institute, Daejeon 34133, Republic of Korea

[2] Rotary-Wing Flight Performance Team, Korea Aerospace Industries, Sacheon 52529, Republic of Korea

[3] Electromechanical Technology, LORD Corporation, Cary, NC 27511-7923, USA

generally not used in newer helicopters that have variable-speed rotors.

The active vibration reduction technique was also attempted in the same way as the passive vibration reduction approach. The first approach was considered at the vibration sources. Higher harmonic control (HHC) has been shown to be technically feasible [5], but it has not yet been applied to commercial aircraft, as it requires a great deal of power and the actuator is a safety critical component. The other active control techniques to vibration sources include trailing edge flaps [6], active twists [7], and active tabs [8], but there is no related commercialized product. Apart from applying active techniques at vibration sources, local vibration control was tried to cancel out the main rotor-induced vibrations in the fuselage, which directly affects humans. In the 1990s, Westland introduced ACSR (Active Control of Structural Response) [9] technology for W-30 helicopters, and it is currently in production on the AW101. Since the 2000s, active vibration control systems (AVCSs) using accelerometers and force generators were demonstrated or commercialized to helicopters such as UH-60, UH-60M, ALH Dhruv, EC225/725, EC135/145, EC130 and Bell 429 [10–17]. The application of AVCS is increasing, and researches on applying this system to the rotor hub have been going on [18].

AVCS can provide similar steady-state vibration reduction compared to the performance of using the passive vibration system; it can also provide significant improvements in transient vibration reduction, weight, and the maintenance cost compared to the passive alternatives. By modularity design in both hardware and software, AVCS is highly flexible to be customized and fitted to different types of helicopter and helicopter configurations.

Basically, when applying AVCS to a helicopter, it is possible to obtain better vibration reduction performance by a large number of sensors and actuators, but it is essential to configure an optimal combination using limited number of sensors and actuators considering weight and cost restrictions. Through the numerical optimization process, potential AVCS configurations exhibited that good predicted performance can be derived and the final AVCS configuration can be determined through parameter adjustment process during the flight tests.

This paper presents a technology demonstration program designed to find a general process solution for mitigating the rotorcraft N/rev tonal vibration issue. This program was collaborated by Korea Aerospace Industries (KAI), LORD, and Korea Aerospace Research Institute (KARI). LORD designed AVCS system [19] and KUH were selected as the performance validation platform for the program. KAI conducted ground and flight tests and KARI conducted its own analysis following LORD's optimization process. The general process solution includes three phases. The first phase is to obtain the helicopter system dynamics and baseline (control off) vibration level in the hanger as well as at various flight conditions, respectively. The second phase is to investigate the phase-one data and predict the vibration performance with the AVC on numerically. An optimization is performed in this phase also to find out the potential AVCS configurations which are used in phase three. The AVCS configuration includes the variety of number of actuators, the actuator command force locations, force orientations, spin directions, maximum force capacities, number of accelerometers, the accelerometer measurement locations and orientations. The final phase is the helicopter tuning flights and performance evaluation flights campaign. In this paper, the performance comparison between the AVCS and the passive TVA (Tuned Vibration Absorber) is presented, and the weight reduction is also illuminated.

2 Active Vibration Control System

2.1 System Architecture

LORD AVCS consists of up to 14 accelerometer sensors, one central controller, and up to 12 CFG actuators. The architecture of the system is shown in Fig. 1. Accelerometers are used for the airframe vibration measurement; the central controller calculates the control input based on the vibration measurement and provides the control input to the CFGs. Then, the actuator generates the forces to perform the vibration control. A tachometer is required to provide the information of the main rotor rotating speed and the blade position to the central controller as a reference signal; this is critical because the vibration of the fuselage is in conjunction with the rotation of the main rotor. The signal buses can be monitored by an external computer.

LORD Circular Force Generator operation diagram is shown in Fig. 2 [19]. Two eccentric masses are rotating at blade-passing speed to generate a circular force whose direction changes periodically. The magnitude of the force can be controlled by adjusting the relative angle of the two disks. It is also possible to operate both imbalance masses in either clockwise or counterclockwise direction with respect to the

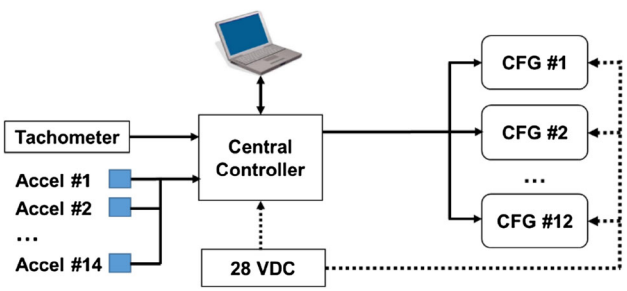

Fig. 1 LORD AVCS architecture

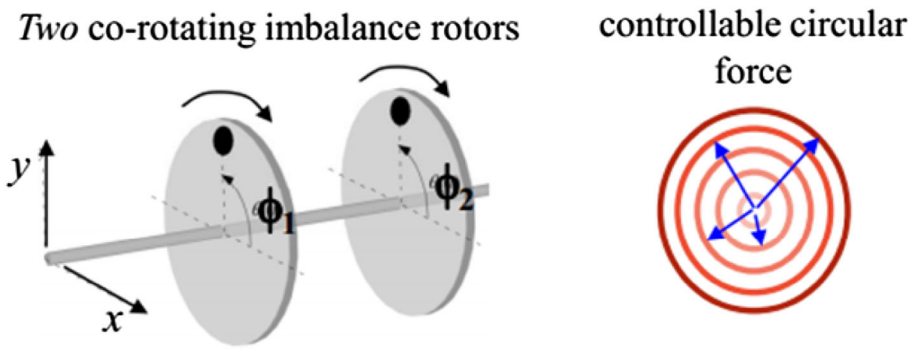

Fig. 2 LORD Circular force generator [19]

axis of rotation. It generates greater force at high operating frequencies because it uses centrifugal force of eccentric masses. The maximum force generated by the CFG depends on the imbalance authority and the squared angular frequency [19].

2.2 Application Process

The general process solution for applying AVCS to a helicopter vibration problem is shown in Table 1. To determine the final configuration of the AVCS, the candidate locations for accelerometers and CFGs are pre-selected in phase 1. The candidate location selections are based on the performance requirements and test interested locations. The accelerometers and the CFGs should be mounted at locations where the responses of the vibration measurement and transmission of the generated force are effectively monitored. The system transfer function acquisition in phase 1 is performed on ground; the task is to measure and analyze the accelerometer responses to the commanded CFG inputs at normal CFG operation conditions. Baseline vibration data acquisition is the process of measuring the vibration level generated for each flight condition without vibration control treatment. Aircraft weight changes, center of gravity of the aircraft, and flight conditions should be considered in phase 1 task to reflect the various vibration conditions that can occur during helicopter operations. In this study, two aircraft weight conditions, operating weight and maximum take-off gross weight were examined. 16 flight test conditions were tested including level flight, deceleration, acceleration, bank turns, climb, descent, and approach. The maximum candidate locations for CFG mounting were identified as 8 locations in the cockpit area and rear cabin area as shown in Fig. 3. Each CFG can be operated in either clockwise (CW) or counterclockwise (CCW) directions; so, it can be considered as 16 actuator configurations.

Figure 4 shows that 45 accelerometer positions including different measurement locations and orientations were selected for system model evaluation. And additional accelerometers were used for monitoring purpose at the engine, gearbox, horizontal tail, and vertical tail.

Table 1 AVCS application process

Phase	Tasks
1	Airframe system transfer function acquisition Baseline flight vibration data acquisition
2	AVCS configuration optimization
3	AVCS tuning and performance evaluation

Potential optimal AVCS configurations are analyzed in phase 2. In phase 3, the final AVCS configuration and control parameter settings are determined through the tuning flight; after flight test data analysis, the performance flight tests are performed to evaluate the final AVCS configuration which can meet all the customer performance requirements.

3 AVCS Optimization

3.1 Algorithm

In many commercial AVCSs, Fx-LMS (filtered-x least mean square) algorithm [20–22] is used and the schematic diagram of this algorithm is shown in Fig. 5. Control command, u, is calculated by the control algorithm using the reference signal, x, measured from the tachometer. The error signal, e, is measured by the accelerometers. The baseline vibration, y, is canceled by $\hat{y}$ generated by the actuator. Here, C^* represents the dynamic characteristics of the forward path, i.e., actuators. The C is the transfer function model obtained from the ground test.

The error signal is the sum of the baseline vibration and the vibration generated by the CFGs as follows:

$$e = \hat{y} + y = C^*u + y \approx Cu + y. \quad (1)$$

Fig. 3 CFG locations

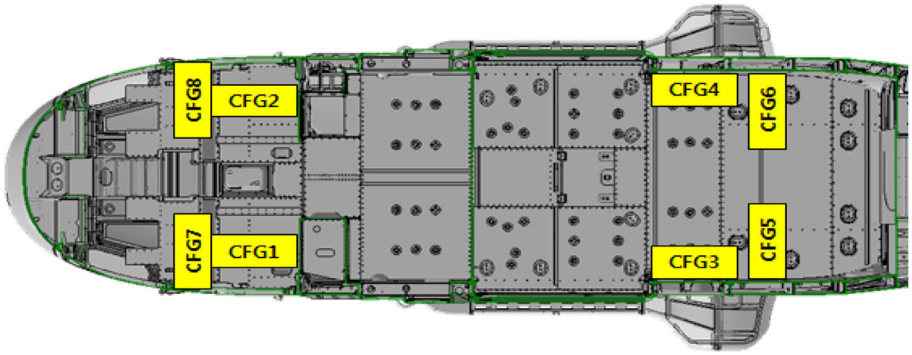

Fig. 4 Accelerometer locations

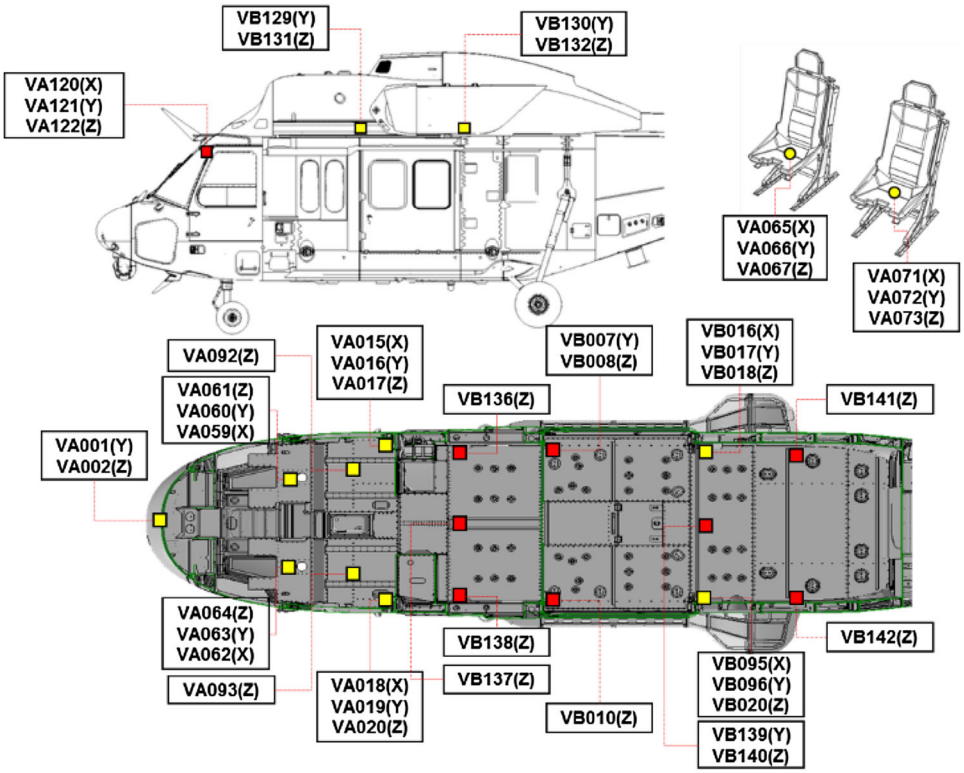

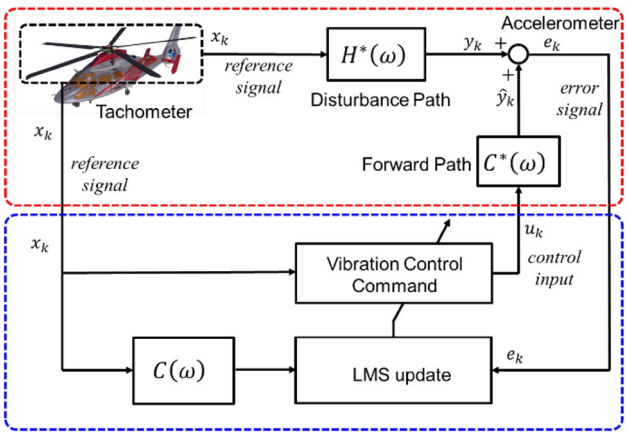

Fig. 5 Fx-LMS algorithm

Vibration reduction means minimizing the magnitude of the error signal. Thus, the objective function can be defined as follows:

$$J = e^{\mathrm{H}} Q e, \tag{2}$$

where Q is the sensor weighting matrix. The optimal control input minimizing the objective function can be calculated as follows:

$$u_{\mathrm{opt}} = -(C^{\mathrm{H}} C)^{-1} C^{\mathrm{H}} Q y. \tag{3}$$

The expected controlled vibration level when AVCS is applied can be calculated by substituting the optimal control input of Eq. (3) into Eq. (1). In actual implementation of the control algorithm, the control input is calculated and applied

using a gradient descent for each time step the controller is driven:

$$u_{k+1} = u_k - \frac{1}{2}\mu\left(\frac{\partial J_k}{\partial u_k}\right), \tag{4}$$

$$\left(\frac{\partial J_k}{\partial u_k}\right) = 2C^{\mathrm{H}}(\omega)Qe_k, \tag{5}$$

$$u_{k+1} = u_k - \mu C^{\mathrm{H}}(\omega)Qe_k, \tag{6}$$

where μ is the step size, and ω is frequency. The forward path transfer function, $C^*(\omega)$, and disturbance path dynamics, $H^*(\omega)$, change according to the excitation frequency. To cope with changes in the vibration characteristics of the aircraft due to the rotor speed change, it is necessary to consider the system including the operational frequency bands.

3.2 Optimization Objective, Constraints, and Process

The sensor and actuator placement optimization process correspond to phase 2 of the AVCS application process described in Table 1. The optimization objective is to choose an optimal AVCS configuration with optimized cost function at the selected accelerometer locations. The optimization constraints in this study are listed as follows.

1. Maximum number of CFG configurations including different CFG locations, orientations, and spin directions, is 6.
2. Due to the AVCS hardware measurement channel limitation, 14 control accelerometer positions are chosen.
3. Maximum CFG force output is constrained to stay within available CFG limits.

Increasing the number of actuators will improve the AVCS performance by effectively reducing the vibration level, but at the same time, the number of actuators should be reduced to minimize the weight and cost of the aircraft. Therefore, the process of optimizing sensor and actuator placement is a trade-off between performance and cost.

Optimization is performed on specific aircraft configuration and flight condition first, and then the investigation of the performance of AVCS on different aircraft configurations and flight conditions are performed during phase 3 shown in Table 1.

The optimization procedure used in this study is shown in Fig. 6.

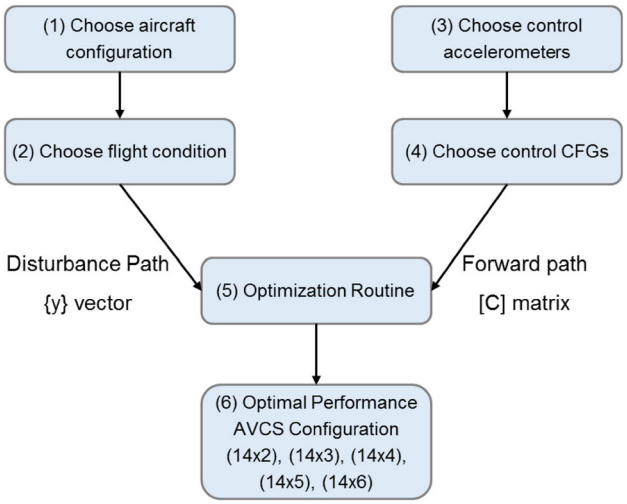

Fig. 6 Optimization analysis procedure

1. By evaluating the baseline flight vibration-level measurement from phase 1, the shapes of vibration level profile of the operating weight and the profile of the maximum take-off gross weight for different flight conditions were similar. The worst vibration level was located in the operating weight; therefore, the operating weight was selected as baseline aircraft configuration for the optimization.
2. KUH showed a pretty good vibration performance in the high-speed range, between 80 and 140 kts. But, vibration level increased at lower speed range. 40-kts level flight condition was chosen as the baseline flight condition for the optimization. It was easy to repeat and relatively fair comparison in the optimization analysis was possible.
3. In phase 1, 45 vibration monitor positions were used for accelerometer data acquisition. The full optimization test matrix of this large number of accelerometer combination will be more than 100 billion, $C(45, 14)$. In the optimization simulation of this study, optimizing the accelerometer locations were not explored; instead, a subjective judgment was made to choose 14 control accelerometers from 45 measurement positions. There were three criteria to choose the control accelerometers,
   (i) Customer required vibration reduction regions.
   (ii) Selected control accelerometer locations should be evenly distributed throughout the selected aircraft regions.
   (iii) The measured vibration levels should be large enough, about 0.2 g, based on the phase 1 baseline flight test measurement.
   The final control accelerometers used in the optimization are shown in the Fig. 7, and the main target areas of the vibration reduction are the cockpit and the rear cabin.
4. Different numbers of actuator test cases were evaluated in this study; test groups 2, 3, 4, 5, and 6 CFGs were chosen from the 8 candidate locations shown in Fig. 3. Two spin directions of each CFG, CW and CCW, were also considered. For 2 CFGs case, possible number of combi-

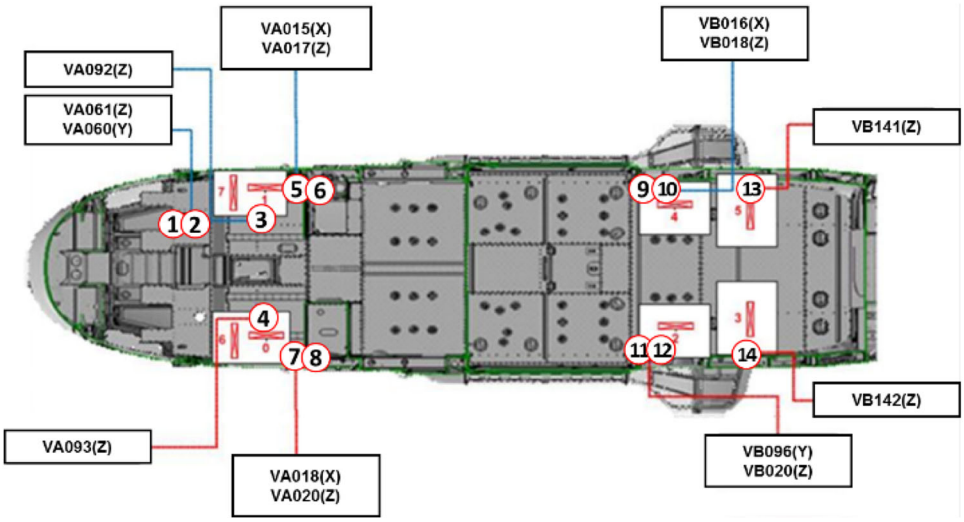

Fig. 7 Control accelerometer set

nation, selecting 2 out of 16, $C(16,2)$, is 120. However, a specific CFG cannot rotate in CW and CCW directions at the same time. Considering this constraint, total 112 combinations are possible for selecting 2 CFGs out of 8 locations. Similar analysis was applied to the other test groups. All possible combinations of CFGs were evaluated for optimization.

5. In the optimization process, an exhaustive simulation test approach was chosen and the predicted AVCS performance was sorted in all test groups of (14×2), (14×3), (14×4), (14×5), and (14×6) configurations. The $(m \times n)$ configuration means m-accelerometers and n-CFGs. For this study, only 1-dimensional control accelerometer was chosen for the flight test. Disturbance path vector was chosen according to the aircraft configuration and the flight condition selection, and the forward path transfer function was selected based on the control accelerometer and CFG configurations. The calculation of the error signal, objective function, and the optimal control input is defined in the Eqs. (1), (2), and (3) defined in Algorithm section, respectively.
6. Top 10 AVCS configurations were selected based on the smallest predicted objective function values in each test group, (14×2), (14×3), (14×4), (14×5), and (14×6) configurations. The objective function represented the square sum of the vibration magnitude measured by 14 accelerometers. Therefore, vibration level at a specific location could be different even though the objective function had the same magnitude. The flight candidate AVCS configurations were selected among the top 10 performance cases, and the final candidate configurations were selected by qualitative evaluation along with the quantitative evaluation during the tuning flight test. Then, the final AVCS configuration was used to perform the evaluation flights.

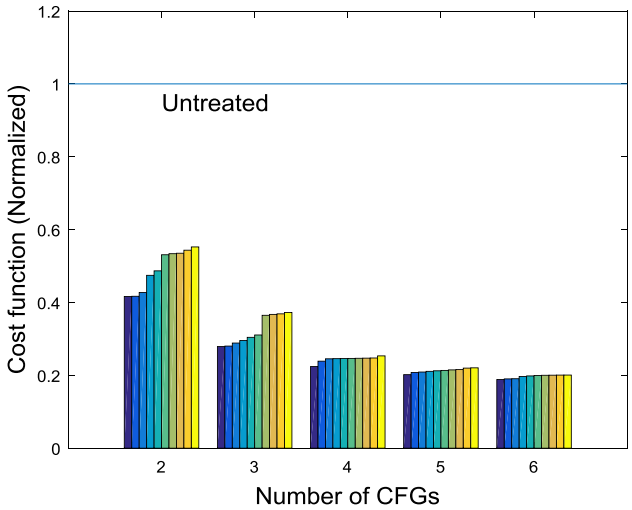

Fig. 8 Vibration reduction performances with respect to the number of CFGs

4 Optimization Results and Discussion

4.1 Effects of the Number of Actuators

The cost function values of top 10 performance test cases in each of test groups of (14×2), (14×3), (14×4), (14×5) and (14×6) systems are shown in Fig. 8. The cost function values were normalized to the value of untreated case.

It can be seen that as the number of CFG increases, the vibration reduction performance increases also, but the performance improvement is slowed down when the number of CFG is more than 5. If the vibration reduction performance below a certain level is expected, an additional vibration reduction will require more number of actuators to be used, which will result in increasing weight and cost.

The vibration levels of the 14 control accelerometers according to the top 10 candidates in each test group are shown in Fig. 9. In each graph, the vertical axis represents the acceleration magnitude normalized to the required vibration limit of cabin area at 40-kts forward flight condition, and the same normalization factor was applied to all figures from 9 to 17. The horizontal axis represents the number of accelerometers, and the ten bars indicate the top 10 performance test cases in each test group shown in Fig. 8 from left to right, and the dotted line represents the normalized vibration without control.

More vibration reduction was achieved as increasing the number of CFGs in the overall aspect. Increasing the number of CFGs from 2 to 3 improves overall vibration reduction performance, but vibration level at 12th location increases. That means the selected CFGs of top 10 performance test cases in (14×3) test group do not have much control authorities. Similarly, (14×2) test group showed low control authorities on accelerometer 14. However, these two accelerometers are representative sensors for the real left cabin area which is one of the customer-required vibration reduction regions. Clearly, increasing the number of CFGs from 3 to 4 improves overall vibration reduction performance including accelerometer 12 and 14. It can be seen that vibration control is possible with an average of 0.1 g when 5 or more CFGs are used. However, when applying AVCS to actual aircraft, total system weight, space required for mounting, power consumption as well as performance should be considered by the customer.

4.2 Analysis of Flight Test AVCS Configuration

Flight test candidate AVCS configurations were selected by considering the vibration reduction performance and system weight among the top 10 performance tests. Tuning flight tests were performed by selecting several combinations of (14×4), (14×5), and (14×6) AVCS configurations with relatively high vibration reduction performance. The flight test results included quantitative accelerometer and CFG control force measurements as well as qualitative evaluations by pilots, co-pilots, and flight test engineers. One (14×5) AVCS configuration was selected as final performance flight test. In addition, one flight test was also conducted on a (14×8) system to see the performance effect of using all KUH possible CFG locations. The final AVCS configuration performance evaluation was the case using the CFG1 (CCW), CFG2 (CW), CFG3 (CW), CFG4 (CCW), and CFG5 (CW) which is shown in Fig. 3.

For the final flight test (14×5) AVCS configuration, the vibration control performance at 40-kts level flight condition was examined through time-domain analysis. The AVCS was simulated to turn the control on at 10 s, and the control input was calculated based on Eq. (6) at each time step using $\mu =$ 0.05. Untreated vibration, control command of CFG3 out of 5 actuators, and controlled vibration at control accelerometer number 2 out of 14 sensors are shown in Fig. 10. The vibration level was normalized to the same value used in Fig. 9, and the force command was normalized to the maximum force output capability of the CFG. The simulation results show that the transient of the vibration reduced was about 1 s after the controller is turned on.

The magnitude of the vibration level calculated by the optimal solution and the gradient descent time domain simulation are compared in Fig. 11. The bar graph shown as 'Optimization analysis' represents the magnitude of the vibration calculated by substituting the optimal control input of Eq. (3) into Eq. (1), and the bar graph labeled as 'Transient analysis' is the steady-state vibration level after the control algorithm is converged as shown in Fig. 10. It can be seen that the magnitude of the steady-state vibration calculated by the time-domain simulation is almost the same as the predicted vibration level of the optimal solution.

During the optimization and transient analyses, saturation of force command was taken into account. If the calculated command force exceeds the maximum allowable CFG limit, output command was saturated. In transient analysis, CFG3 showed maximum force as shown in Fig. 10.

The vibration levels at all 45 accelerometer positions including 14 control accelerometers are shown Fig. 12. The 14 control accelerometers are marked in red with circled number. It can be seen that the vibration levels of most other accelerometer locations are also reduced, even though they are not used for control accelerometers. However, vibration level increased in some accelerometer locations including no. 20 and 43. Therefore, to check the vibration characteristics of the entire aircraft, it is important to monitor the vibration level not only at the control accelerometer locations but also at all the interested locations.

The final task for the flight test configuration is to tune the weightings. It is possible to adjust weights of actuators and sensors simultaneously, but only the effects of sensor weights are presented in this paper. Performance evaluation was performed under unit weighting condition for the optimization process in phase 2. Accelerometer weights tuning was carried out during flight tests to adjust local vibration levels to meet the aircraft vibration-level performance requirements and reflect qualitative evaluation requirements by pilots and co-pilots. To enhance the vibration reduction performance at accelerometers 3 and 4 locations in z-direction at the pilot and co-pilot floors, accelerometer weights were adjusted for accelerometers 3 and 4. Figure 13 shows the effects of the accelerometer weight tuning. The third bar graph indicates the simulation result of weight tuning, and the fourth bar graph shows the magnitude of the vibration measured in the final evaluation flight test. The simulation result is very close

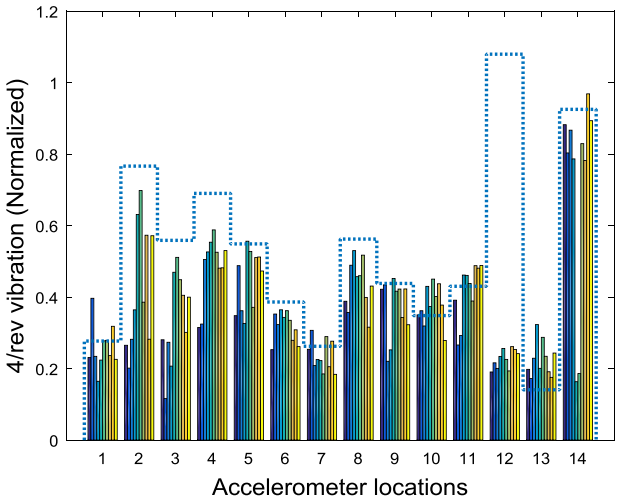

(a) 14x2 system

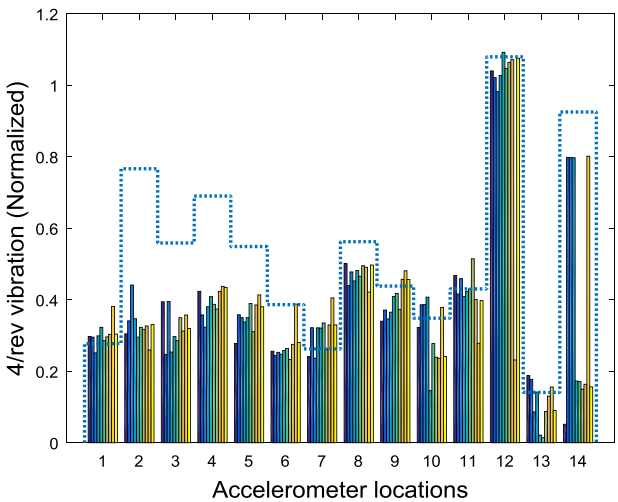

(b) 14x3 system

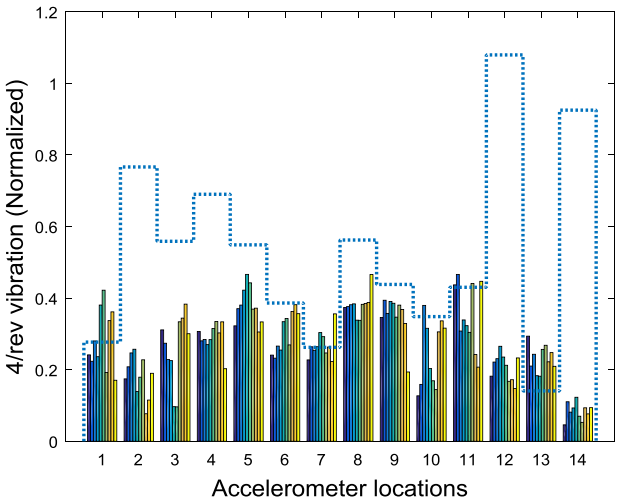

(c) 14x4 system

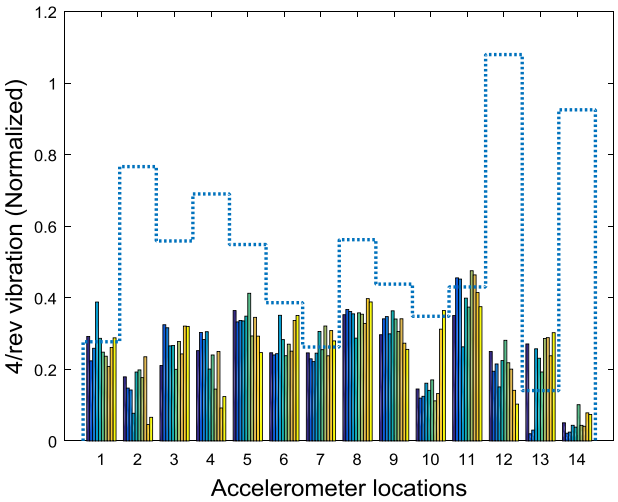

(d) 14x5 system

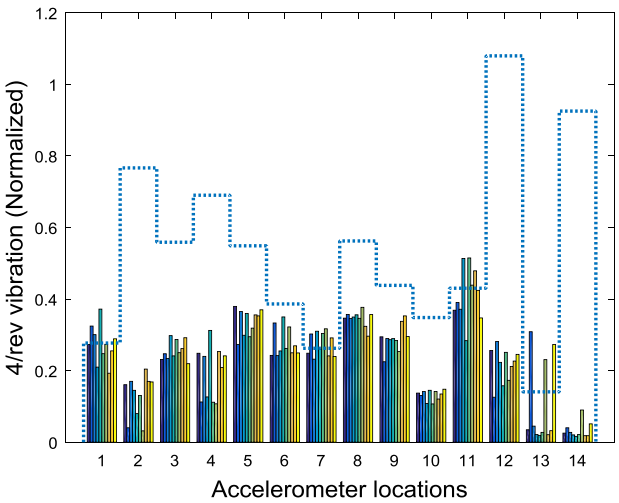

(e) 14x6 system

Fig. 9 Vibration reduction performances for all test groups

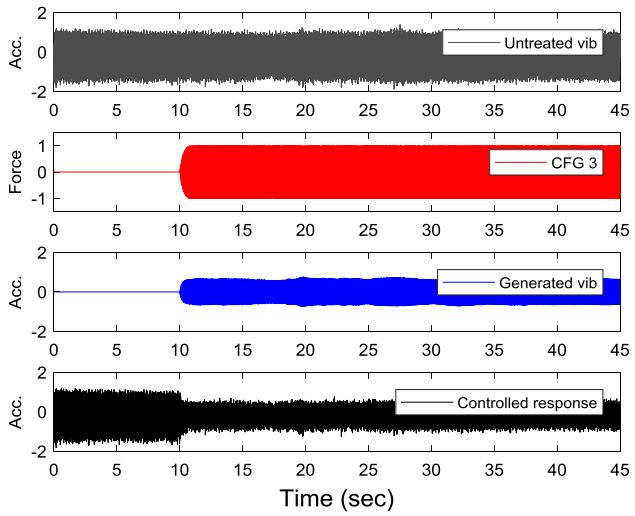

Fig. 10 Time-domain simulation using (14×5) AVCS configuration

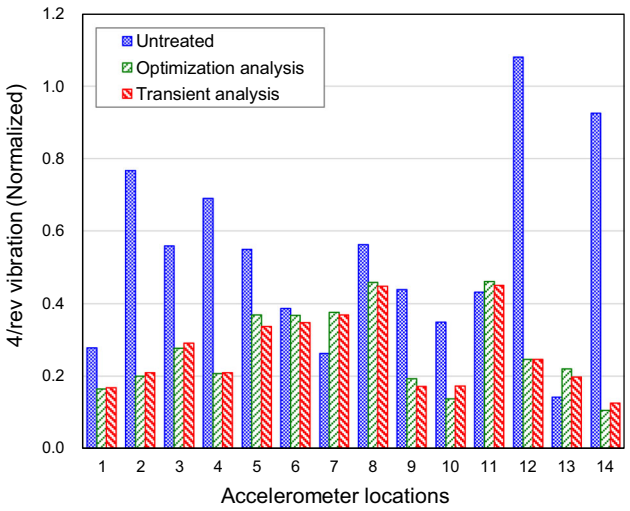

Fig. 11 Comparison of optimal solution and time domain simulation result

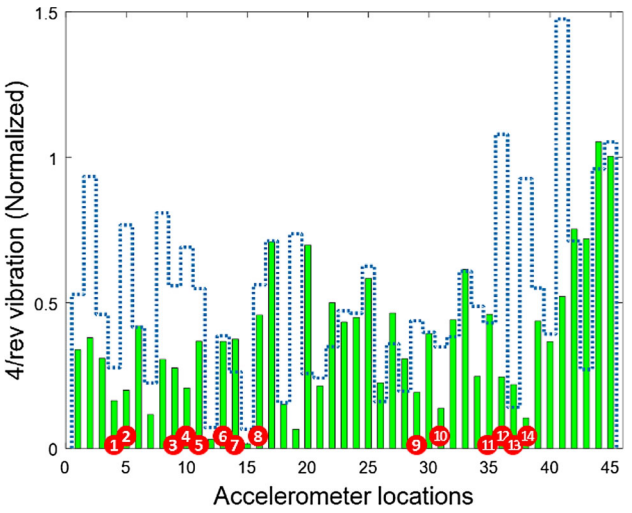

Fig. 12 Vibration reduction performances at 45 locations for (14×5) test group

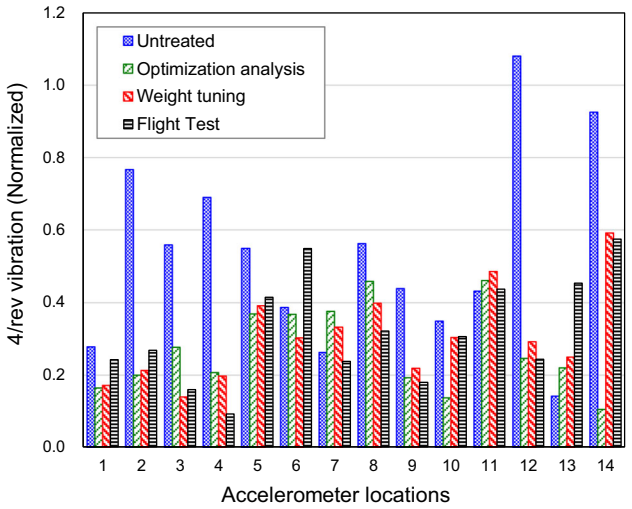

Fig. 13 Effects of accelerometer weight tuning and comparison with flight test data

to the flight test result with considering the changes in the flight condition.

4.3 Performance Evaluation Flight Test

The performance evaluation flight test was performed for the final (14×5) and (14×8) AVCS configurations with tuned sensor weights. The magnitude of the z-direction acceleration signals at the pilot heel position and the co-pilot heel position among the 45 accelerometers is shown in Fig. 14. By applying AVCS, the average vibration level was reduced by about 70% compared to the baseline vibration level, and 40–50% more vibration reduction was obtained compared with the case of using a passive tuned vibration absorber (TVA). In the case of applying 8 CFGs, additional vibration reduction effect was not significant compared to the case of using 5 CFGs in level flight conditions. The vibration level of the z-direction at the cabin real floor left-hand side was also reduced by more than 80% compared to the baseline vibration level and exhibited superior vibration reduction performance compared to TVA as shown in Fig. 15. TVAs were installed on the floor of cockpit area and left-hand side of cabin frame as shown in Fig. 16.

The transient performance of AVCS was also explored. During the flight condition change from low speed level flight to approach, a high level of vibration occurred instantaneously around 20-kts speed; which is around 4 s in Fig. 17. Although TVA was not effective during the approach, AVCS showed comparatively superior performance compared to that of the TVA as shown in Fig. 17.

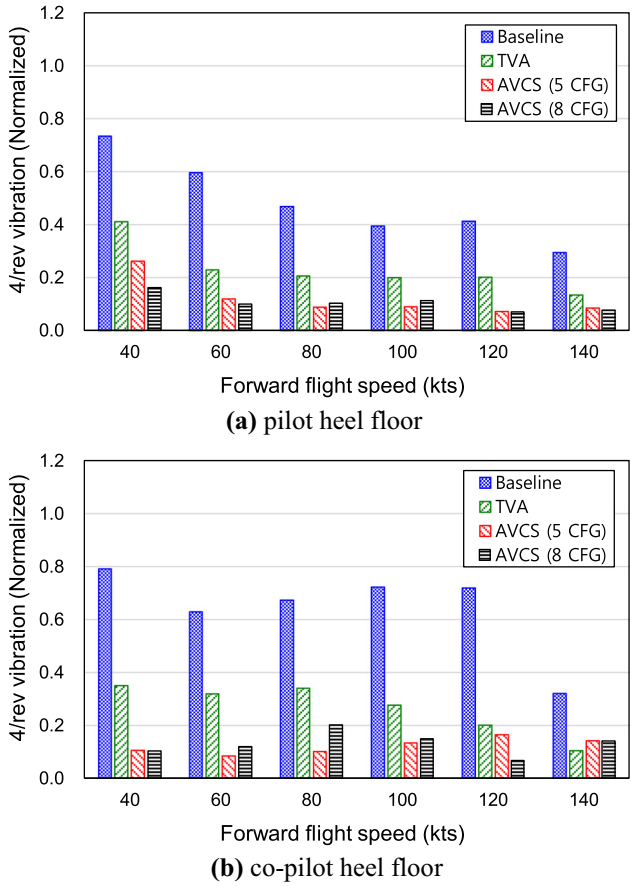

Fig. 14 Vibration levels at pilot/co-pilot heel floor z-direction

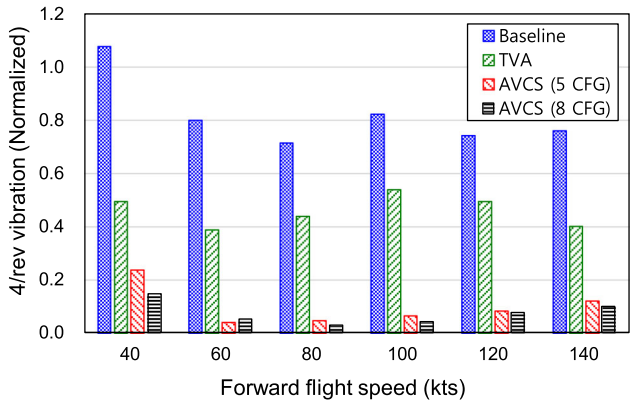

Fig. 15 Vibration levels at cabin rear floor left hand side z-direction during level flight

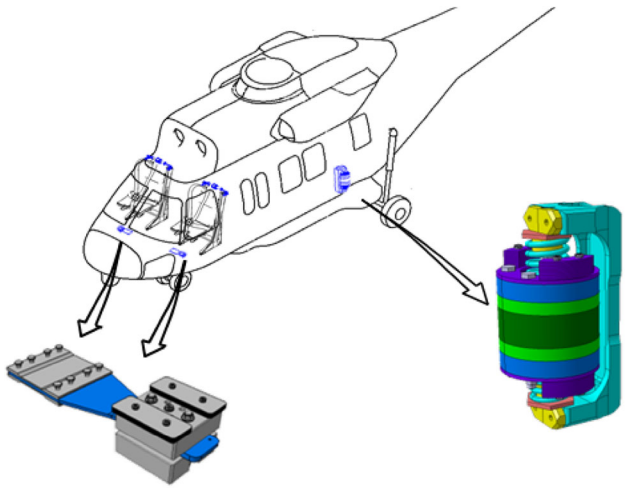

Fig. 16 Locations of tuned vibration absorbers

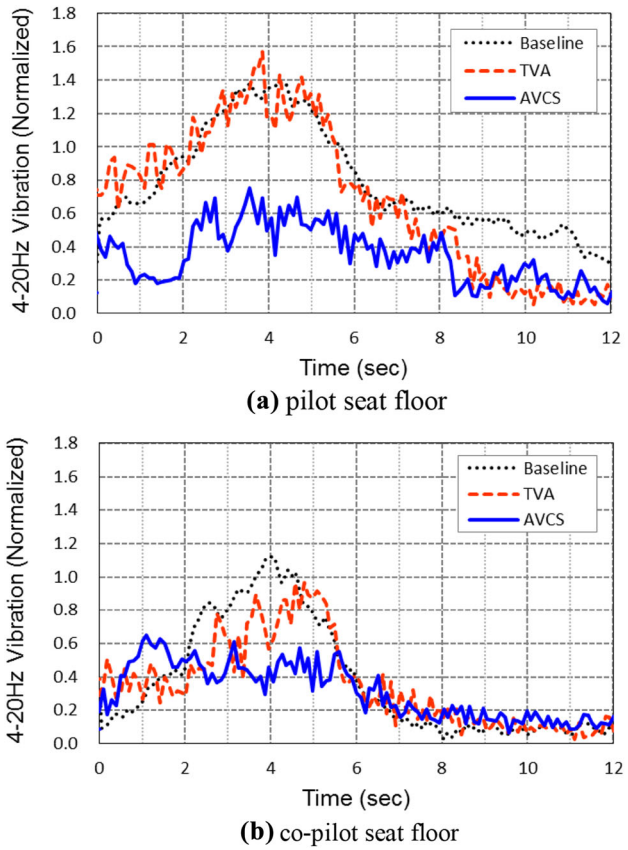

Fig. 17 Vibration level at pilot/co-pilot seat floor locations during approach

4.4 AVCS Weight Comparison

The total weight of the five CFGs in the AVCS for the performance demonstration program is 66% of the total weight of TVA applied to the existing KUH platform. Even including the controller, accelerometers, and the cables required for AVCS, it is still possible to configure a lighter weight of AVCS with better vibration reduction performance than the passive TVA system. In (14×8) AVCS configuration, the weight is slightly higher than the weight of the TVA; so, there is no weight-saving effect in comparison with the vibration reduction performance enhancement. For the KUH, it is appropriate to construct a (14×5) AVCS configuration based on the flight test results of this study. Although the final

system configuration depends on the user's choice, it seems possible to replace the passive vibration reduction device with the AVCS with better performance and lower weight.

5 Conclusion

In this study, LORD AVCS product performance was demonstrated on KUH platform.

A systematic process was applied to find a vibration reduction solution. The suggested optimization process consists of three phases. The first phase is to obtain the helicopter system dynamics and baseline vibration level. The second phase is to predict the vibration performance with the AVC on numerically. An optimization is performed in this phase to find out the potential AVCS configurations which are used in phase three. The final phase is the helicopter tuning flights and the performance evaluation flights. Systematic optimization process is a very useful approach even when the dimension of the helicopter system model is large.

The flight test results showed that the AVCS successfully suppressed the cockpit area and cabin area floor vibration level compared with the baseline vibration level for various flight conditions. Vibration level was reduced by more than 70% compared to the baseline vibration at level flight condition, and 40–50% more vibration reduction was achieved than conventional TVA. AVCS also showed superior performance than TVA during the transient condition at approach. Moreover, weight saving was also achieved.

Acknowledgements This study was supported by the LCH Core Technology Development Program (Project number: 10053157) funded by the Ministry of Trade, Industry and Energy, Republic of Korea.

References

1. Loewy RG (1984) Helicopter vibrations: a technological perspective. J Am Helicopter Soc 29(4):4–30
2. Reichert G (1980) Helicopter vibration control—a survey. In: 6th European rotorcraft and powered lift aircraft forum, Bristol, England, Sep 16–19, 1980
3. Yun CY, Kim DH, Kang HJ (2013) Vibration prediction of helicopter airframe. In: 2013 KSNVE annual spring conference, Yeosu, April 25–26, 2013
4. Jung SU, Kwak DI, Kim SH, Choi J, Shim DS (2013) Vibration reduction devices for korean utility helicopter. J Korean Soc Aeronaut Sp Sci 41(12):987–993
5. Splettstoesser WR, Heller H, Mercker E, Preisser JS, Yu YH (1995) The HART programme, a quadrilateral cooperative research effort. In: 51st AHS annual forum, Fort Worth, Texas, May 9–11, 1995
6. Milgram J, Chopra I, Straub F (1998) Rotors with trailing edge flaps: analysis and comparison with experimental data. J Am Helicopter Soc 43(4):319–332
7. Lim JW, Boyd DD Jr., Hoffmann F, van der Wall BG, Kim DH, Jung SN, You YH, Tanabe Y, Bailly J, Lienard C, Delriuex Y (2014) Aeromechanical evaluation of smart- twisting active rotor. In: 40th European rotorcraft forum, Southampton, U.K., Sep 2–5, 2014
8. Kim DH, Kang HJ, Wie SY, Kim SH (2013) Modeling of a rotor system incorporating active tab and analysis of BVI noise reduction characteristics. J Korean Soc Aeronaut Sp Sci 41(11):855–864
9. Staple AE (1990) An evaluation of active control of structural response as a means of reducing helicopter vibration. In: 46th AHS annual forum, vol 1, Washington, D.C., May 21–23, 1990, pp 3–17
10. Welsh W, Fredrickson C, Rauch C, Lyndon I (1995) Flight test of an active vibration control system on the UH-60 Black Hawk helicopter. In: 51st AHS annual forum, Fort Worth, Texas, May 9–11, 1995
11. Millott T, Goodman R, Wong J, Welsh W, Correia J, Cassil C (2003) Risk reduction flight test of a pre-production active vibration control system for the UH-60M. In: 59th AHS annual forum, Phoenix, Arizona, May 6–8, 2003
12. Heilmann J, Swanson D, Badre-Alam A, Narayana Rao KS (2003) Vibration attenuation through the use of active Frahms. In: 59th AHS annual forum, Phoenix, Arizona, May 6–8, 2003
13. Vignal B, Kryzinski T (2005) Development and qualification of active vibration control system for the EC225/EC725. In: 61st AHS annual forum, Grapevine, Texas, June 1–3, 2005
14. Konstanzer P, Enenkl B, Aubourg PA, Cranga P (2008) Recent advances in Eurocopter's passive and active vibration control. In: 64th AHS annual forum, Montreal, Canada, April 29–May 1, 2008
15. Hoffmann F, Konstanzer P, Priems M, Chemin J (2009) Active cabin vibration reduction for jet-smooth helicopter ride. In: 35th European rotorcraft forum, Hamburg, Germany, September 22–25, 2009
16. Priems M, Kerdreux B, Dreher S, Jouve J, Marrot F, Reymond M (2012) Vibration comfort improvement through active vibration control and its certification on EC130T2. In: 38th European rotorcraft forum, Amsterdam, Netherlands, Sep 4–7
17. Mahmood R, Heverly D II (2012) In-flight demonstration of active vibration control technologies on the bell 429 helicopter. In: 68th AHS annual forum, Fort Worth, Texas, May 1–3
18. Andrews J, Welsh W, Altieri R, DiOttavio J (2014) Ground and flight testing of a hub mounted vibration suppression system. In: 70th AHS annual forum, Montreal, Quebec, Canada, May 20–22, 2014
19. Swanson D, Black P, Girondin V, Bachmeyer P, Jolly M (2015) Active vibration control using circular force generator. In: 41st European rotorcraft forum, Munich, Germany
20. Elliott SJ, Nelson PA (1993) Active noise control. In: IEEE signal processing magazine, pp 12–35
21. DJolly MR, Rossetti DJ, Southward SC (1995) On actuator weighting in adaptive control systems. In: DSC-Vol. 57-2, IMECE proceedings of the ASME dynamic systems and control division, ASME 1995, pp 843–852
22. Jolly MR, Rossetti DJ, Southward SC (1994) Actuator redundancy in adaptive control systems. In: DE-vol. 75, active control of vibration and noise, ASME 1994, pp 19–24